

Exchange bias in manganite/SrRuO₃ superlattices

M. Ziese, F. Bern, and I. Vrejoiu

Citation: *J. Appl. Phys.* **113**, 063911 (2013); doi: 10.1063/1.4790877

View online: <http://dx.doi.org/10.1063/1.4790877>

View Table of Contents: <http://jap.aip.org/resource/1/JAPIAU/v113/i6>

Published by the [American Institute of Physics](#).

Related Articles

Continuous-film vs. device-level ferromagnetic resonance in magnetic tunnel junction thin films
J. Appl. Phys. **113**, 083903 (2013)

Reducing the writing field of L10-FePt by graded order parameter
J. Appl. Phys. **113**, 073912 (2013)

Enhanced inverse spin-Hall effect in ultrathin ferromagnetic/normal metal bilayers
Appl. Phys. Lett. **102**, 072401 (2013)

Heat-induced damping modification in yttrium iron garnet/platinum hetero-structures
Appl. Phys. Lett. **102**, 062417 (2013)

Effect of antiferromagnetic thickness on thermal stability of static and dynamic magnetization of NiFe/FeMn multilayers
J. Appl. Phys. **113**, 063913 (2013)

Additional information on *J. Appl. Phys.*

Journal Homepage: <http://jap.aip.org/>

Journal Information: http://jap.aip.org/about/about_the_journal

Top downloads: http://jap.aip.org/features/most_downloaded

Information for Authors: <http://jap.aip.org/authors>

ADVERTISEMENT



AIP Advances

Now Indexed in
Thomson Reuters
Databases

Explore AIP's open access journal:

- Rapid publication
- Article-level metrics
- Post-publication rating and commenting

Exchange bias in manganite/SrRuO₃ superlattices

M. Ziese,¹ F. Bern,¹ and I. Vrejoiu²

¹*Division of Superconductivity and Magnetism, University of Leipzig, D-04103 Leipzig, Germany*

²*Max Planck Institute of Microstructure Physics, D-06120 Halle, Germany*

(Received 14 December 2012; accepted 22 January 2013; published online 13 February 2013)

The magnetization processes in Pr_{0.7}Ca_{0.3}MnO₃/SrRuO₃ and La_{0.7}Sr_{0.3}MnO₃/SrRuO₃ superlattices were studied. In both superlattices the ferromagnetic layers are antiferromagnetically coupled across the interfaces. Whereas superlattice La_{0.7}Sr_{0.3}MnO₃/SrRuO₃ showed a three-step magnetization reversal mechanism for all temperatures, superlattice Pr_{0.7}Ca_{0.3}MnO₃/SrRuO₃ had a compensation point with a two-step below and a three-step reversal mechanism above the compensation temperature. Exchange-bias and coercive fields, the vertical magnetization shift as well as the minor loop opening were measured as a function of the cooling field. Main findings were a change of the exchange-bias field from negative to positive values for increasing cooling fields in the two-step reversal regime and from negative values to zero for increasing cooling fields in the three-step reversal regime. Exchange-bias training occurs mostly within the first magnetization cycle. The data are consistent with the formation of interfacial domain walls. © 2013 American Institute of Physics. [<http://dx.doi.org/10.1063/1.4790877>]

I. INTRODUCTION

Magnetization curves of exchange-coupled magnetic layers might show a horizontal shift along the magnetic field axis. The magnitude of this shift, the exchange-bias field, not only depends on material parameters but also on the magnetic state of the layers. As an example, a dependence of the exchange-bias field on the magnitude of the cooling field was reported.^{1–3} Further, the exchange bias shows a training effect, i.e., a dependence on the number of magnetization cycles the magnetically soft ferromagnetic component has undergone.^{4–8} Depending on the particular system: ferromagnetic-antiferromagnetic⁴ or ferromagnetic-ferromagnetic^{5–7} and on the particular spin structure,^{9–11} different mechanisms are responsible for the training effect. However, a common feature of these mechanisms is the dependence of exchange-bias training on the interfacial spin-structure. Therefore, an analysis of exchange-bias training should yield information on the latter. The aim of this work is to study the interfacial spin states of manganite/SrRuO₃ superlattices by measuring the dependence of the exchange-bias field on the cooling field, the magnetic hysteresis procedure and the training. These oxide systems are of particular interest, since the interfaces are atomically sharp.¹² Moreover, individual layers with a defined thickness of only a few unit cells can be coherently grown, such that there are only very few coupled spins across the thickness of a single layer.

La_{0.7}Sr_{0.3}MnO₃ (LSMO)/SrRuO₃ (SRO) bilayers and superlattices (SLs)^{13–17} as well as Pr_{0.7}Ca_{0.3}MnO₃ (PCMO)/SRO superlattices¹⁸ show antiferromagnetic (AF) interlayer coupling and positive exchange bias. The exchange-bias strength depends sensitively on intermixing, structural defects and the insertion of nonmagnetic interlayers at the interface.^{16,17,19} Tuning the intricate interplay between structure, magnetocrystalline anisotropy, AF interlayer coupling, magnitude of the layer magnetization and layer thickness allows for the fabrication of samples with two types of

magnetization reversal mechanisms: conventional two-step (soft layer first, hard second) as well as more exotic three-step (hard layer first, followed by reversal of the ferrimagnetic SL state, hard third) reversal processes.^{17,19} For the present work two samples were chosen: (i) a LSMO/SRO superlattice with a three-step magnetization reversal and (ii) a PCMO/SRO superlattice with a two-step magnetization reversal below a compensation temperature and a three-step magnetization reversal above that temperature.

II. EXPERIMENTAL

The superlattices were fabricated by pulsed laser deposition (KrF laser) onto slightly vicinal SrTiO₃ (001) substrates with a miscut angle of about 0.1°, uniform TiO₂-termination and an atomically flat terrace morphology. Substrate temperature was 650 °C and oxygen partial pressure 0.14 mbar. The microstructure of the SLs was studied by transmission electron microscopy (TEM), atomic force microscopy, and X-ray diffractometry; extensive structural characterization can be found in Refs. 12, 16–19. Both samples consist of 15 bilayers; the LSMO/SRO SL has layer thicknesses of 4 (LSMO) and 8 (SRO) unit cells, the PCMO/SRO SL of 4 (PCMO), and 11 (SRO) unit cells.

The magnetic properties of the SLs were measured by SQUID magnetometry; the magnetic field was applied parallel to the layers. Reproducibility of the measurements was about 10⁻⁷ emu, resolution about 2 × 10⁻⁸ emu. The magnetic moments were normalized to the total SL volume to obtain an average magnetization. Full hysteresis loops were measured after zero field cooling between ±7T, the maximum attainable field in the SQUID. Minor loops between ±B were measured following two protocols. In the first protocol, the SLs were cooled from 200 K in a cooling field B_{FC} to the respective measuring temperature; subsequently the minor hysteresis loop was measured. In the second protocol, the SLs were zero-field cooled to the respective measuring

temperature; then a magnetic field of +7 T was applied to saturate the SL in the positive field direction, followed by the measurement of the minor loop. In case of training effect measurements, minor loops were repeated three to five times in consecutive fashion. We followed the standard procedure and defined the exchange-bias field B_x by the horizontal shift of the magnetization hysteresis-loop of the soft ferromagnetic component, when this loop is traversed without re-magnetizing the hard ferromagnetic component. Technically this hysteresis loop is a full hysteresis loop of the soft ferromagnetic component, but a minor hysteresis loop of the SL. Remanence measurements were made either after field cooling, removing the field at 5 K and measuring on warming in zero field (RemH) or after stabilizing at a temperature, ramping to +7 T and back to 0 T and measuring at that particular temperature (RemT). Strictly, the measurements were not done in zero field, but in the remanent field of the superconducting solenoid.

III. RESULTS

Selected magnetization data of SL LSMO/SRO are shown in Fig. 1. The full hysteresis loop in Fig. 1(a)

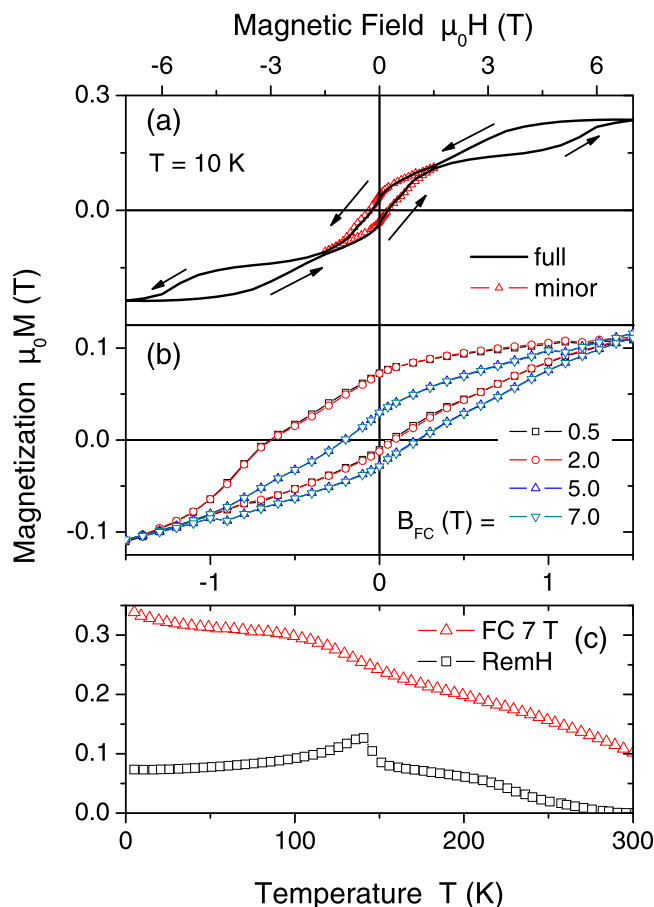


FIG. 1. Magnetization data of sample LSMO/SRO. (a) Full hysteresis loop and minor loop with field amplitude of 1.5 T at 10 K. The minor loop was measured after ZFC and subsequent application of +7 T (protocol 1). (b) Minor loops measured after FC in B_{FC} at 10 K (protocol 2). (c) FC magnetization in 7 T and remanent magnetization (RemH) as a function of temperature. The remanence was measured after FC in +7 T and removing the field at 5 K.

indicates three magnetization reversals: at low magnetic fields the SL forms a ferrimagnetic structure that is reversed by reversing the field; at high magnetic fields the magnetically hard SRO layers are slowly rotated toward the field direction.¹⁷ Note that at 10 K the maximum field of 7 T available in the SQUID might not be sufficient to fully saturate the magnetization, since there is a small horizontal shift of the central loop of +0.017 T at this temperature. The full hysteresis loop at 10 K has necks at 1.5 T; at this temperature, however, it is difficult to clearly define the central minor loop that is to be used for the exchange-bias effect measurements. Therefore minor loops with amplitudes of 1.0 and 1.5 T were measured; one minor loop between ± 1.5 T (protocol 2) is shown in Fig. 1(a). On this field scale no obvious horizontal or vertical shifts of the minor loop are discernable. At higher temperatures the separation between low and high field loops is much clearer and the central minor loop could be clearly defined. In Fig. 1(b) minor loops recorded at 10 K after field cooling in B_{FC} (protocol 1) are shown on a smaller field scale. Whereas a clear left-shift of the minor loops was found for cooling fields up to about 2 T, the minor loops are almost centered for higher cooling fields. The temperature dependent magnetization curves in Fig. 1(c) show the ferromagnetism in both LSMO and SRO layers as well as the antiferromagnetic interlayer coupling in the remanent state.¹⁶

Selected magnetization data of SL PCMO/SRO are shown in Fig. 2. A full hysteresis and a minor loop (protocol 2) at 10 K are presented in Fig. 2(a). In contrast to SL LSMO/SRO the hysteresis shows a two-step magnetization reversal with the magnetically soft PCMO layer reversing first in low fields and the magnetically hard SRO layer reversing in high fields of opposite polarity.¹⁷ Since the interlayer coupling is antiferromagnetic, this leads to an inverted central hysteresis loop, see also Refs. 17 and 18. Minor loops measured after cooling in a field B_{FC} (protocol 1) are presented in Fig. 2(b). For small cooling fields a left-shift, for larger cooling fields a right-shift of the loops is seen. Figure 2(c) shows the magnetization of the SL in an applied field of 7 T as well as the remanent magnetization measured after the SL was first saturated in +7 T at each measurement temperature. Below a compensation temperature of 22 K the remanence is negative corresponding to inverted hysteresis loops. Above 22 K the hysteresis loops of this sample are similar to those of SL LSMO/SRO.

The minor loops recorded after FC in various cooling fields B_{FC} showed three characteristics, namely: they are shifted (a) horizontally and (b) vertically and (c) all loops are open, i.e., the first and last point of the loops measured at maximum positive field do not agree. In order to make this observation more quantitative the exchange-bias field is defined by the zero crossings of the magnetization as

$$B_x = \frac{B_{c+} + B_{c-}}{2}, \quad (1)$$

where B_{c-} and B_{c+} denote the coercive fields on the down- and up-going hysteresis branch. The coercive field is defined as

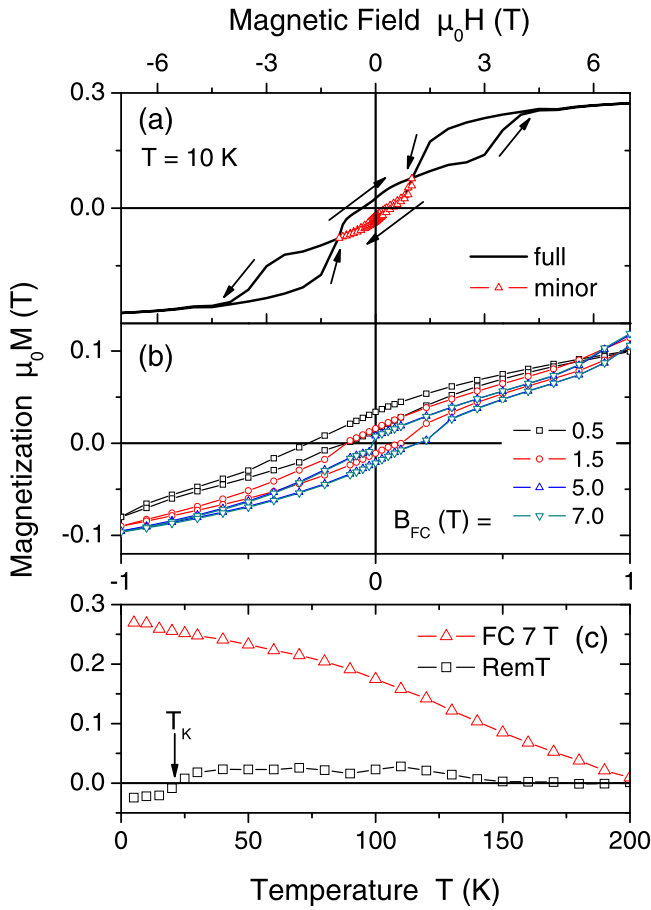


FIG. 2. Magnetization data of sample PCMO/SRO. (a) Full hysteresis loop and minor loop with field amplitude of 1.0 T at 10 K. The minor loop was measured after ZFC and subsequent application of +7 T (protocol 1). (b) Minor loops measured after FC in B_{FC} at 10 K (protocol 2). (c) FC magnetization in 7 T and remanent magnetization (RemT) as a function of temperature. The remanence was recorded after application and removal of +7 T at each measurement temperature.

$$B_c = \frac{B_{c+} - B_{c-}}{2}. \quad (2)$$

The relative vertical magnetization shift is defined by

$$m_V = \frac{(M_{1+} + M_{l+}) + 2M_-}{(M_{1+} + M_{l+}) - 2M_-}, \quad (3)$$

where M_{1+} , M_{l+} , and M_- denote the magnetization values of the first, last, and reversal point of the minor hysteresis loops. The relative loop opening is defined by

$$\Delta m = \frac{4(M_{1+} - M_{l+})}{(M_{1+} + M_{l+}) - 2M_-}. \quad (4)$$

Exchange-bias and coercive fields, vertical magnetization shifts and loop openings were determined for both samples as a function of cooling field B_{FC} (protocol 1). Measurements were carried out for both samples at 10 and 50 K, respectively. Figs. 3 and 4 show the resulting data at 10 K. The data at 50 K of both samples show a similar trend to the 10 K data, see Fig. 4 for SL PCMO/SRO.

The dependence of the exchange-bias B_x and coercive B_c fields as a function of cooling field B_{FC} can be seen in

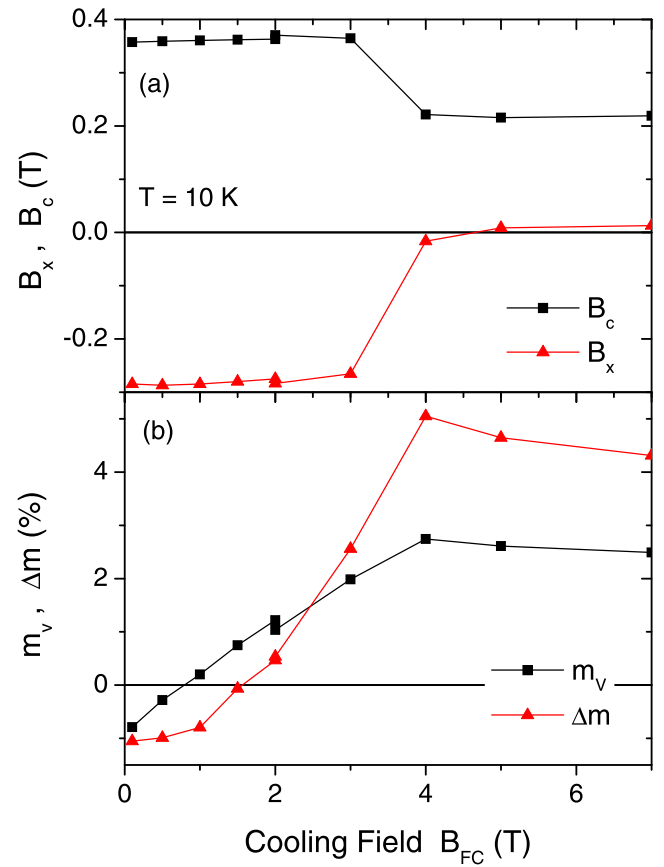


FIG. 3. SL LSMO/SRO at 10 K: (a) Exchange bias B_x and coercive field B_c as well as (b) relative vertical magnetization shift m_V and loop opening Δm as a function of cooling field B_{FC} (protocol 1).

Figs. 3(a) and 4(a). For both SLs a distinct cooling field dependence was observed: the exchange bias field is negative at low cooling fields, whereas at 10 K it approaches zero (LSMO/SRO) or +80 mT (PCMO/SRO) above crossover fields of 3.5 and 1.6 T, respectively. The crossover fields have values close to the centers of the hard layer magnetization loops, see Figs. 1 and 2. It is important to notice that B_x approaches zero at large cooling fields for sample LSMO/SRO at all temperatures studied and for sample PCMO/SRO for temperatures above the compensation temperature $T_K = 22$ K. Below T_K the exchange bias field approaches a finite value. This is consistent with the shape and interpretation of the full hysteresis loops. In sample PCMO/SRO below the compensation temperature, the soft layer is reversed with the hard layer keeping its magnetization direction; in this standard magnetization process the exchange-bias field can be measured as a horizontal shift of the soft layer. In SL PCMO/SRO above the saturation temperature and in SL LSMO/SRO at all temperatures, the central loop corresponds to the reversal of a ferrimagnetic layer state; a horizontal loop shift of this state might be related to the formation of interfacial domain walls. The coercive field B_c has an anomaly near the crossover field, either a jump or a peak. The data are reminiscent of data on a Fe/FeF₂ bilayer² and a GdFe/TbFe superlattice.³ A similar behaviour was also reported in Ref. 20 apart from the fact that the authors showed the absolute value of the exchange-bias field, thus

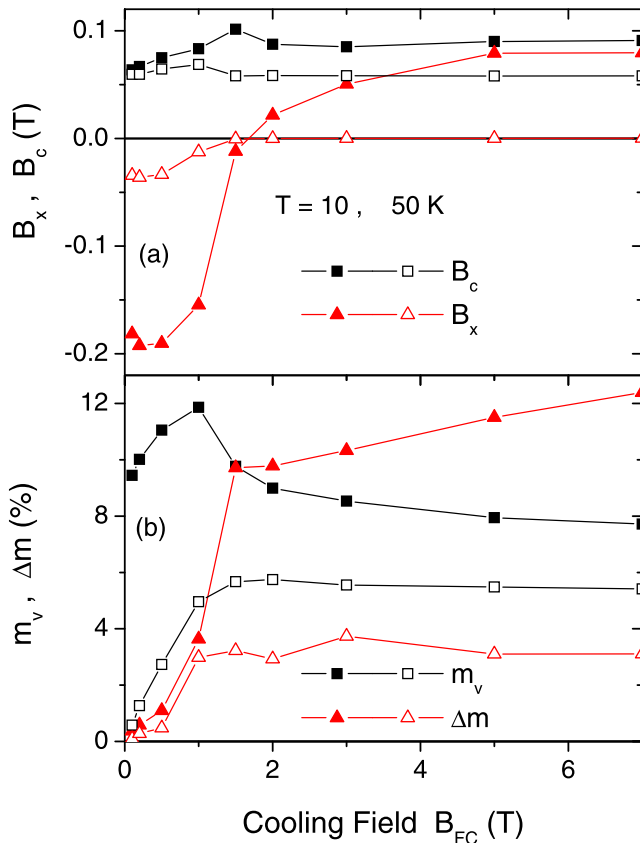


FIG. 4. SL PCMO/SRO at 10 K (solid symbols) and 50 K (open symbols): (a) Exchange bias B_x and coercive field B_c as well as (b) relative vertical magnetization shift m_V and loop opening Δm as a function of cooling field B_{FC} (protocol 1).

missing the negative B_x values at low cooling field as well as the zero crossing. The B_x and B_c data show that the exchange-bias field is not only determined by the Mn–O–Ru coupling strength but also by the detailed interfacial magnetization state.

The vertical magnetization shift and the loop openings are shown in Figs. 3(b) and 4(b). For both SLs a systematic variation with the cooling fields was found. Whereas the vertical loop shift m_V increases with cooling field in case of SL LSMO/SRO at all temperatures and SL PCMO/SRO at 50 K, it is essentially constant for SL PCMO/SRO at 10 K. The loop openings Δm show an increase with increasing cooling field for both samples, i.e., after cooling in a large field the minor loop is open with the last measured magnetization value below the first one. Note that the variation of B_c and Δm for SL PCMO/SRO has the same trend at 10 K and 50 K, although the character of the hysteresis loop changes from inverted to non-inverted. This shows that these parameters are not characteristics of the magnetization reversal mechanism, but of the interfacial spin states. However, the magnetization reversal-mechanism changes the behaviour of the apparent exchange-bias field B_x : below the compensation temperature T_K this approaches a finite exchange-bias field at large cooling fields, whereas above T_K it approaches zero at large cooling fields.

Figure 5 shows the exchange-bias field B_x and the loop opening Δm as a function of the number of consecutively measured hysteresis loops. A small training effect of the

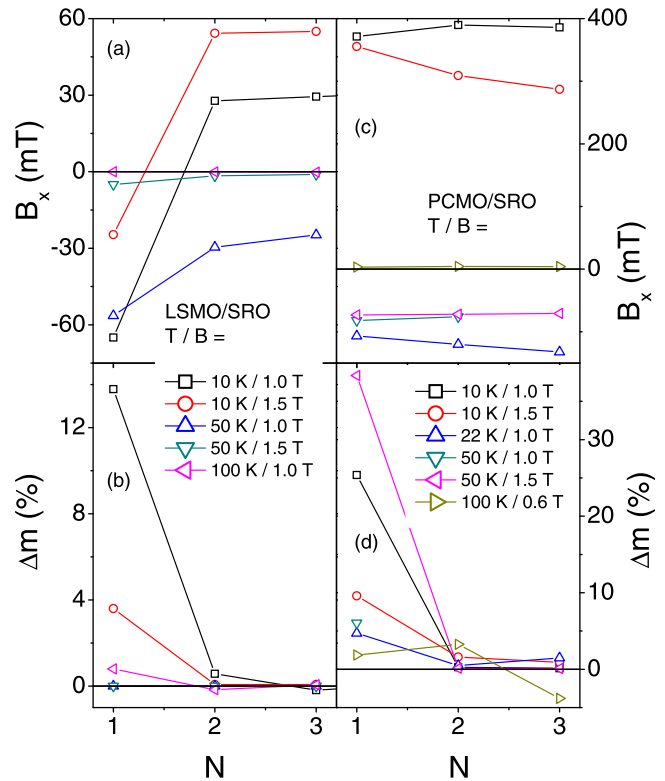


FIG. 5. (a,c) Exchange bias field and (b) and (d) relative loop opening as a function of the loop number $N = 1, 2, 3$. Data were obtained for both samples with protocol 2. Data obtained after field cooling show the same trend. B denotes the amplitude of the minor loop with the field being swept between $\pm B$.

exchange-bias field was observed; also the loop opening decreases in consecutive hysteresis loops. The training effect occurs mostly within the first minor loop, since from the second loop onward the variation of both B_x and Δm is close to the field resolution (10^{-4} T) and magnetic moment reproducibility (10^{-7} emu) of the SQUID magnetometer. The training data show that the equilibrium state reached after field cooling is altered by field cycling. We suspect that subsequent field cycling mainly alters the structure of the interfacial domain walls.

On a closer inspection of the Δm training data one finds that the change of the loop opening is especially large in cases, in which the minor loop field range is not chosen in an appropriate way. This is certainly true in case of SL LSMO/SRO at 10 K and a minor loop amplitude $B = 1$ T. This amplitude is too small to ensure a full reversal of the central hysteresis loop such that both B_x and Δm are affected by minor minor-loop effects, i.e., by incomplete traversals of the minor loop. Similar effects in single SrRuO₃ films were also erroneously reported as arising from exchange bias.^{21–23} On the other hand, in case of SL PCMO/SRO at 50 K and $B = 1.5$ T the minor-loop field-amplitude is too large leading to a re-magnetization of the hard SRO layers and therefore also to a large Δm change during the first loop.

IV. DISCUSSION

In this work the dependence of the exchange-bias field, coercive field, vertical magnetization shift and loop opening

of two manganite/SrRuO₃ SLs was studied as a function of the magnetic history, especially as a function of the cooling field and the iteration number of consecutively measured loops. Main findings were a crossover from negative to positive exchange-bias fields for increasing cooling fields as well as a training effect occurring mostly during the first field cycle. The zero crossing of the exchange-bias field was accompanied either by a jump or a maximum in the coercive field. The vertical magnetization shift increases along the field direction for increasing cooling fields, since the spin direction is aligned further with the magnetic field. In general, the minor loops are open, i.e. the last measured magnetization value is smaller than the first. Consecutive cycling of the hysteresis loops leads to a strong decrease of both exchange-bias field and loop opening as well as to some decrease of the vertical magnetization shift. The data are rather similar to data on exchange-coupled Fe/FeF₂ bilayers,^{1,2} Fe/MnF₂ bilayers,^{2,24} CoO coupled to Co-based multilayers²⁵ as well as Gd₄₀Fe₆₀/Tb₁₂Fe₈₈ bilayers.³ This is somewhat surprising, since apart from the samples of Kirk *et al.*²⁵ the bilayers had rather thick layers, typically in the several 10 nm range. In contrast to that, our samples have only four unit cell thick LSMO and PCMO layers, i.e., there are only four manganese spins present across the thickness of a layer.

Although the overall trend of our data agrees with literature data, there is one important difference. Since SL PCMO/SRO shows a two step magnetization-reversal process below the compensation temperature, it is conceptually closer to a system in which a ferromagnetic layer is coupled to an antiferromagnetic one. In both cases the magnetization (or sublattice magnetization) direction of the hard ferromagnet (antiferromagnet) is only weakly affected, when the magnetization of the soft ferromagnetic layer is cycled. In both cases, see Fig. 4(a) and literature data,^{1,2,24} the exchange-bias field varies from negative at low to positive values at high cooling fields. The situation is different in SL LSMO/SRO and in SL PCMO/SRO above the compensation point. In these cases we find a variation of the exchange-bias field from negative at low to zero at high cooling fields, see Figs. 3(a) and 4(a). In contrast, literature results^{3,25} showed an evolution from negative to positive exchange-bias fields (with about the same absolute value) with increasing cooling field. Although in Refs. 3 and 25 the room temperature hysteresis curves showed a similar three-step magnetization reversal as in our samples, we suspect that the low temperature magnetization curves (which are not shown in Refs. 3 and 25), for which the exchange-bias fields were reported, followed a different reversal process.

The exchange bias and its modification with the cooling field was attributed to the presence of interfacial domain walls^{26,27} and the dependence of the spin direction on the cooling field.³ Continuum micromagnetic models usually lead to a good agreement between measured data and calculated magnetization curves or exchange-bias fields.^{3,28} We believe that this explanation also holds for SL PCMO/SRO below the compensation point. Therefore, we conclude that on field cooling interfacial domain walls form in the PCMO/SrRuO₃ SL. These determine the location of the coercive

fields B_{c+} and especially B_{c-} , and therefore of B_x . After field cycling the interfacial domain walls are re-magnetized, leading to an appreciable training effect within the first minor loop as well as to the vanishing of the loop opening Δm . The situation is different in SL PCMO/SRO above the compensation point and in SL LSMO/SRO. Since the interfacial magnetic structure remains the same in SL PCMO/SRO and since it is similar in SL LSMO/SRO, it is likely that formation of interfacial domain walls also occurs. However, since the manganite layers are rather thin having only four spins across their thickness and since the antiferromagnetic coupling is rather large, interfacial domain walls expand into the thicker SRO layers on field reduction. This leads to the three-step magnetization reversal, which is expected to show no horizontal loop shift of the central magnetization loop. This is consistent with the experimental results obtained for high cooling fields. At low cooling fields magnetic domains might be present in the samples and might affect the shape of the minor loops.

The present studies show that interfacial domain walls form at the manganite/SrRuO₃ interface. Although continuum micromagnetic models yield a reasonable description, one would prefer discrete spin models in view of the very few spins present across the thickness of the individual layers. A further theoretical description using ab-initio values for exchange integrals and anisotropy constants remains for future work.

ACKNOWLEDGMENTS

This work was supported by the DFG within SFB 762 "Functionality of Oxide Interfaces". F.B. is member of the Leipzig School of Natural Sciences "BuildMoNa".

- ¹J. Nogués, D. Lederman, T. J. Moran, and I. K. Schuller, *Phys. Rev. Lett.* **76**, 4624 (1996).
- ²J. Nogués, C. Leighton, and I. K. Schuller, *Phys. Rev. B* **61**, 1315 (2000).
- ³S. Mangin, F. Montaigne, and A. Schuhl, *Phys. Rev. B* **68**, 140404(R) (2003).
- ⁴A. Hoffmann, *Phys. Rev. Lett.* **93**, 097203 (2004).
- ⁵C. Binek, S. Polisetty, X. He, and A. Berger, *Phys. Rev. Lett.* **96**, 067201 (2006).
- ⁶S. Polisetty, S. Sahoo, and C. Binek, *Phys. Rev. B* **76**, 184423 (2007).
- ⁷S. Polisetty, S. Sahoo, A. Berger, and C. Binek, *Phys. Rev. B* **78**, 184426 (2008).
- ⁸A. Paul and A. Teichert, *Appl. Phys. Lett.* **97**, 032505 (2010).
- ⁹J. Nogués, T. J. Moran, D. Lederman, I. K. Schuller, and K. V. Rao, *Phys. Rev. B* **59**, 6984 (1999).
- ¹⁰P. Miltényi, M. Gierlings, J. Keller, B. Beschoten, G. Güntherodt, U. Nowak, and K. D. Usadel, *Phys. Rev. Lett.* **84**, 4224 (2000).
- ¹¹J. Keller, P. Miltényi, B. Beschoten, G. Güntherodt, U. Nowak, and K. D. Usadel, *Phys. Rev. B* **66**, 014431 (2002).
- ¹²R. Hillebrand, E. Pippel, D. Hesse, and I. Vrejoiu, *Phys. Status Solidi A* **208**, 2144 (2011).
- ¹³X. Ke, M. S. Rzechowski, L. J. Belenky, and C. B. Eom, *Appl. Phys. Lett.* **84**, 5458 (2004).
- ¹⁴X. Ke, L. J. Belenky, C. B. Eom, and M. S. Rzechowski, *J. Appl. Phys.* **97**, 10K115 (2005).
- ¹⁵P. Padhan, W. Prellier, and R. C. Budhani, *Appl. Phys. Lett.* **88**, 192509 (2006).
- ¹⁶M. Ziese, I. Vrejoiu, E. Pippel, P. Esquinazi, D. Hesse, C. Etz, J. Henk, A. Ernst, I. V. Maznichenko, W. Hergert, and I. Mertig, *Phys. Rev. Lett.* **104**, 167203 (2010).

- ¹⁷M. Ziese, I. Vrejoiu, and D. Hesse, *Appl. Phys. Lett.* **97**, 052504 (2010).
- ¹⁸M. Ziese, I. Vrejoiu, E. Pippel, E. Nikulina, and D. Hesse, *Appl. Phys. Lett.* **98**, 132504 (2011).
- ¹⁹M. Ziese, E. Pippel, E. Nikulina, M. Arredondo, and I. Vrejoiu, *Nanotechnology* **22**, 254025 (2011).
- ²⁰S. N. Jammalamadaka, J. Vanacken, and V. V. Moshchalkov, *Europhys. Lett.* **98**, 17002 (2012).
- ²¹L. Pi, S. Zhang, S. Tah, and Y. Zhang, *Appl. Phys. Lett.* **88**, 102502 (2006).
- ²²L. Klein, *Appl. Phys. Lett.* **89**, 036101 (2006).
- ²³L. Pi, S. Zhang, S. Tah, and Y. Zhang, *Appl. Phys. Lett.* **89**, 039902 (2006).
- ²⁴C. Leighton, J. Nogués, B. J. Jönsson-Åkerman, and I. K. Schuller, *Phys. Rev. Lett.* **84**, 3466 (2000).
- ²⁵T. L. Kirk, O. Hellwig, and E. E. Fullerton, *Phys. Rev. B* **65**, 224426 (2002).
- ²⁶D. Mauri, H. C. Siegmann, P. S. Bagus, and E. Kay, *J. Appl. Phys.* **62**, 3047 (1987).
- ²⁷M. Kiwi, J. Mejía-López, R. D. Portugal, and R. Ramírez, *Europhys. Lett.* **48**, 573 (1999).
- ²⁸R. L. Stamps, *J. Magn. Magn. Mater.* **242–245**, 139 (2002).